Article

Cite This: Biomacromolecules 2018, 19, 3040−3047

pubs.acs.org/Biomac

Single-Chain Glycopolymer Folding via Host−Guest Interactions and Its Unprecedented Effect on DC-SIGN Binding

Gokhan Yilmaz,[†] Veselina Uzunova,[‡] Richard Napier,[‡] and C. Remzi Becer*[,†]

[†]Polymer Chemistry Laboratory, School of Engineering and Materials Science, Queen Mary, University of London, E1 4NS, London, United Kingdom

[‡]Life Sciences, University of Warwick, CV4 7AL, Coventry, United Kingdom

Supporting Information

ABSTRACT: Reversible self-folding actions of natural biomacromolecules play crucial roles for specific and unique biological functions in Nature. Hence, controlled folding of single polymer chains has attracted significant attention in recent years. Herein, reversible single-chain folded glycopolymer structures in α-shape with different density of sugar moieties in the knot were created. The influence of folding as well as the sugar density in the knot was investigated on the binding capability with lectins, such as ConA, DC-SIGN, and DC-SIGNR. The synthesis of triblock glycocopolymers bearing β-CD and adamantane for the host−guest interaction and also mannose residues for the lectin interaction was achieved using the reversible addition−fragmentation chain transfer (RAFT) polymerization technique. The reversible single-chain folding of glycopolymers was achieved under a high dilution of an aqueous solution and the self-assembled folding was monitored by 2D nuclear overhauser enhancement spectroscopy (NOESY) NMR and dynamic light scattering. The lectin binding profiles consistently provided an unprecedented effect of single chain folding as the single-chain folded structures enhanced greatly the binding ability in comparison to the unfolded linear structures.

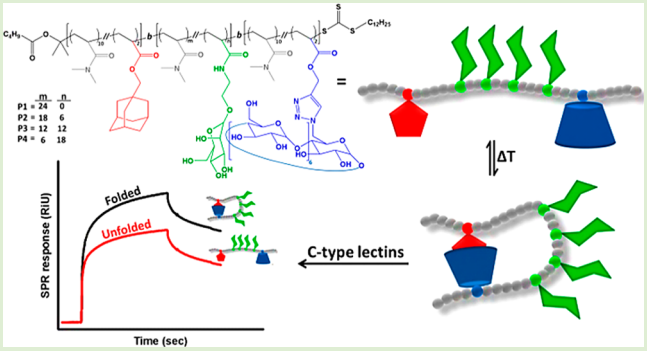

INTRODUCTION

Nowadays, single-chain technology has been elucidated for a deep understanding of the multivalent functions and the precise mechanism of naturally occurring single-chain architectures of macromolecules in biological systems (i.e., tertiary structure of proteins or enzymes).[1−3] In Nature, many biomolecules exhibit reversible self-folding that is necessary for interfacial molecular recognition. Therefore, the development of synthetic single polymers capable of folding precisely into functional supramolecules is an important step forward if we are to create complex macromolecules to imitate the complexity of biological systems. In pursuit of this goal, recent advances in controlled polymerization techniques have allowed polymer chemists to produce precision polymers with controlled chain length, architecture, monomer sequence, chain folding, and tertiary structures.[4−10] However, there remain challenges with defined single-chain collapse and the possibilities offered by controlled folding of single-chain polymers to confer specific biological functions with the precision of naturally occurring polymers.[11]

Single-chain folded polymer structures can be generated via selective point folding or repeat unit folding routes.[12−18] The selective point folding approach can use metal−ligand complexation, host−guest chemistry, hydrogen bonding, and covalent bonding to give relatively controlled architectures with a good folding accuracy.[19−21] The repeat unit folding approach provides less-defined folding structures due to random distribution of functional groups, but it offers a much straightforward synthesis route.[22−25] Very few reports were published on these methodologies in the last five years. For example, Lutz and collaborators have developed a very efficient strategy for fabricating different polymer chain folding architectures (such as P-, Q-, 8-, and α-shaped folding origamis).[17] To achieve this, *N*-substituted maleimides were polymerized with styrene using atom transfer radical polymerization (ATRP) to obtain controlled primary polymer structures. Intramolecular covalent bridges via functional groups positioned on the polymer chain dictated the single-chain folding.

Host−guest interaction is another versatile approach for constructing selective single-chain folding structures.[26−29] In general, host molecules contain a large cavity volume such as cyclodextrins (CD), cucurbiturils (CB) and calixarenes. Typical guest molecules have a complementary shape and interact with the host molecules. Hence, selective noncovalent interactions between the host and the guest molecules confer

Received: April 10, 2018
Revised: May 25, 2018
Published: June 5, 2018

DOI: 10.1021/acs.biomac.8b00600
Biomacromolecules 2018, 19, 3040−3047

order on the molecular system. Recently, Barner-Kowollik and co-workers succeeded in creating reversible, single-chain, selective point polymer folding using a β-cyclodextrin driven host−guest interaction with adamantane in water.[15] Water-soluble poly(*N*,*N*-dimethylacrylamide) carrying β-CD and an adamantyl moiety at the chain ends was synthesized via reversible addition−fragmentation chain transfer (RAFT) polymerization. Folding was followed by dynamic light scattering (DLS) and nuclear overhauser enhancement spectroscopy (NOESY) spectroscopy.

Inspired by these studies, we herein demonstrate a reversible single-chain folding of glycopolymer structures into an α-shape using different density of sugar moieties. Well-defined triblock glycocopolymers carrying different amounts of mannose moieties were synthesized and single-chain folded structures were obtained in an aqueous solution under high dilution, which was monitored by 2D NOESY NMR and dynamic light scattering (DLS) techniques. Glycopolymer architecture, valency, size, and density of binding elements can affect their lectin binding activities significantly. Therefore, folded single-chain glycopolymer structures were evaluated for binding to a series of relevant lectins via the turbidity assay and surface plasmon resonance (SPR) spectrometer. Exciting results were obtained using both binding techniques and three different lectins, which all proved the unprecedented effect of single-chain folding on significantly improved lectin-binding abilities.

EXPERIMENTAL SECTION

Materials. *N*,*N*-Dimethylacrylamide (DMA, 99%, contains 250 ppm mono methyl ether hydroquinone (MEHQ) as inhibitor), *N*-hydroxylethyl acrylamide (97%, contains 1000 ppm MEHQ as inhibitor), β-cyclodextrin (β-CD, 97%), 1-adamantanemethanol (Ad, 99%), *p*-toluenesulfonyl chloride (TsCl, ≥99%), 1-aminoadamantane hydrochloride (≥99%), sodium azide (NaN_3, ≥99.5%), propargyl alcohol (99%), propargyl acrylate (98%), D-(+)-mannose (≥99%), sodium methoxide (CH_3ONa, 25 wt % in methanol) were purchased from Sigma-Aldrich Chemical Co. (Dorset, U.K.). DMA was passed through a short column of basic alumina in order to remove MEHQ inhibitor prior to polymerization. 4,4′-azobis(2-methylpropionitrile) (AIBN), 4,4′-Azobis(4-cyanopentanoic acid) (V-501) and H_2SO_4-silica catalyst were previously synthesized within the group. The RAFT agent, 2-(((dodecylthio)carbonothioyl)thio)propan-2-yl pentanoate, kindly provided by Lubrizol. ConcanavalinA (ConA) was also purchased Sigma-Aldrich Chemical Co. (Dorset, U.K.). All other reagents and solvents were obtained at the highest purity available from Sigma-Aldrich Chemical Co. (Dorset, U.K.) and used as received unless stated otherwise. Water (H_2O, HiPerSolv Chromanorm for HPLC from VWR International, U.K.) was used throughout the study. Dialysis tubes were purchased from Spectrum Laboratories (California, U.S.A.).

Instrument and Analysis. Proton and carbon-13 (^1H and ^{13}C NMR) nuclear magnetic resonance spectroscopy (Bruker DPX-400/600) were used to determine the chemical structure of the synthesized polymers. Samples were dissolved at 5 mg/mL concentration in D_2O, $(CD_3)_2SO$, and $CDCl_3$ solvents depending on the solubility of the samples.

DOSY experiments were performed on a 400 MHz Bruker Avance III spectrometer equipped with a broadband ^1H decoupling probe (PABBO) using an Eddy current compensated bipolar gradient pulse sequence (BPLED) at a temperature of 298 K. Proton pulse lengths were determined to be 11.15 μs and bipolar gradients of δ = 4.8−6.4 ms. Eight scans with 12k complex data points were recorded for each increment with 8 dummy scans per experiment, leading to an overall experiment time of 20 min and 31 s per sample. The diffusion delay Δ was set to 100 ms. Corresponding diffusion coefficients *D* of the polymer signals and the solvent are the result of the fitting procedure, which was performed by using Topspin 3.1 software.

2D NOESY NMR experiments were performed on a 600 MHz Bruker Avance III spectrometer at a temperature of 295 or 340 K. The mixing time was set to 200 μs. The 90° pulse was determined to be 8.7 μs. Spectra were recorded with 4k × 1k complex data points using 16 or 20 scans per t1 increment and 16 dummy scans at 25 and 70 °C. The spectral width was set to 5 × 5 ppm which leads to a total experiment time of between 5 and 7 h. After zero filling to 4k × 2k points and apodization, using a 90°-phase shifted squared sine function, the spectra were Fourier transformed.

Size-exclusion chromatography (SEC) measurements were conducted on an Agilent 1260 infinity system operating in DMF with 5.0 mM NH_4BF_4 and equipped with refractive index detector (RID) and variable wavelength detector (VWD), 2 PLgel 5 μm mixed-C columns (300 × 7.5 mm), a PLgel 5 mm guard column (50 × 7.5 mm), and an autosampler. The instrument was calibrated with linear poly(methyl methacrylate) standards in range of 550 to 46890 g·mol^{-1}. All samples were passed through 0.2 μm PTFE filter before analysis.

The mean hydrodynamic diameters (D_h, the volume weight diameter of the distribution) were determined by using a Malvern Zetasizer Nano ZS instrument equipped with a He−Ne laser at 633 nm. DLS measurements were performed by taking 1 mL of nanoparticle solution from the dialyzed solution directly. All measurements were carried out at 25 and 70 °C and repeated three times.

UV−visible spectra were recorded on a PerkinElmer Lamda 25 UV/vis spectrometer equipped with a (PTP-1) temperature control unit at a certain temperatures in the range of 200 and 600 nm using quartz microcuvettes.

GC was used to measure monomer conversion of DMA and AdAc. GC analysis was performed using an Agilent Technologies 7820A. An Agilent J&W HP-5 capillary column of 30 m x 0.320 mm with a film thickness of 0.25 mm was used. The oven temperature was programmed as follows: 40 °C (hold for 1 min) increase at 30 °C/min to 300 °C (hold for 2.5 min). The injector was operated at 250 °C and the FID was operated at 320 °C. Nitrogen was used as carrier gas at flow rate of 6.5 mL/min and a split ratio of 1:1 was applied. Chromatographic data was processed using OpenLab CDS ChemStation Edition, version C.01.05.

The FT-IR spectra were recorded on a Bruker FT-IR spectrometer TENSOR II with Diamond-ATR module. The scanning range was 600−4000 cm^{-1} and the resolution was 1 cm^{-1}.

Matrix assisted laser desorption/ionization-time-of-flight mass spectroscopy (MALDI-ToF MS) was performed using a Bruker Daltonics Autoflex MALDIToF mass spectrometer, equipped with a nitrogen laser at 337 nm with positive ion ToF detection. *trans*-2-[3-(4-*tert*-Butylphenyl)-2-methyl-2-propenylidene]malononitrile (DCTB, ≥98%) and potassium trifluoroacetate (KTFA) were used as matrix and cationisation agent, respectively. Spectra were recorded in reflectron mode and the mass spectrometer was calibrated with a peptide mixture up to 6000 Da.

Methods. *Synthesis of D-Mannose Acrylamide Glycomonomer (ManAcm).* D-Mannose pentaacetate (6.73 g, 0.017 mol) and *N*-hydroxylethyl acrylamide (2.22 g, 0.019 mol) were dissolved in anhydrous dichloromethane (25 mL) and then degassed by argon gas for 10 min. Subsequently, boron trifluoride diethyl etherate (8.63 g, 0,060 mol) was added via syringe and the solution was sonicated for 90 min. The reaction solution was washed with brine for 3 times (30 mL). After the organic layer was dried over $MgSO_4$, the solvent was removed under reduced pressure to obtain a yellowish gummy crude product. The obtained crude product was used directly without any further purification to synthesize 2-(D-manosyloxy) hydroxylethylacrylamide. The protection of acetyl groups was carried out in the presence potassium carbonate (1.0 g, 7.2 mmol) in methanol (25 mL). The reaction was followed by thin-layer chromatography (TLC). After the neutralization of the reaction solution using Amberjet 1200H (H^+) cation exchange resin. The resin was removed by filtration and the solvent was removed under reduced pressure. The obtained crude product was purified by column chromatography (chloroform/MeOH), gradient elution) to yield a white amorphous solid upon lyophilizing (0.67 g, yield: 32.6%).

DOI: 10.1021/acs.biomac.8b00600
Biomacromolecules 2018, 19, 3040−3047

^{1}H NMR (D_2O, 298 K, 400 MHz): δ 6.32 (dd, 1H, J = 14.6 Hz, CH_2), 6.30 (dd, 1H, J = 14.2 Hz, CH), 5.82 (dd, 1H, J = 14.4 Hz, CH), 5.12 (m, 1 H, H-1 of mannose), 4.82 (t, 2H, CH_2−OH), 4.22 (m, 2 H, CH_2−NH), 3.82 (t, 2H, CH_2−CH_2), 3.40−3.82 (m, H residues of mannose) ppm. ^{13}C NMR (D_2O, 298 K, 400 MHz): δ 152.3 (C═O), 134.7 (C−CH_2), 126.5 (N−CH═C), 105.9 (C 1 of mannose), 72.3, 71.1, 69.6, 68.3 (carbons of anomeric mannose), 64.7 (CH_2−NH), 28.3 (CH_2−CH_2), 19.7 (CH_2−OH) ppm. ESI-MS m/z: Calcd for $C_{11}H_{19}NO_7$ ($M + H^+$), 277.2; found, 277.1.

Synthesis of Adamantane Acrylate Monomer (AdAc). 1-Adamantane methanol (3.0 g, 18.0 mmol) as dissolved in 80 mL of THF and Et_3N (6.3 mL, 45.0 mmol) was added. The reaction mixture was then cooled to 0 °C. Acryloyl chloride (1.7 mL, 21.6 mmol) in THF (20 mL) was added dropwise within 30 min. The reaction mixture was stirred for 15 min at 0 °C then overnight at room temperature. The reaction was filtered off, solvent was evaporated and was added CH_2Cl_2, then extracted with HCl (1 M, 2 × 30 mL), deionized water (2 × 30 mL) in sequence. After removing the solvents by a rotary evaporator, the crude product was purified by column chromatography over silica gel eluting with hexane/EtOAc (9/1; yield = 2.9 g, 73%).

^{1}H NMR ($CDCl_3$, 298 K, 400 MHz): δ 6.33 (d, 1H, J = 16.9 Hz, CH_2), 6.06 (dd, 1H, J = 17.3 Hz, CH), 5.74 (d, J = 10.4 Hz, 1H, CH_2), 3.89 (s, 2H, CH_2O) 1.92 (m, 3H, CH), 1.70 and 1.65 (d, 6H, CH_2), 1.60 (d, 6H, CH) ppm. ^{13}C NMR ($CDCl_3$, 298 K, 400 MHz): δ 167.2 (C═O), 131.4 (C−CH_2), 128 (CH═C), 72.4 (CH_2O), 39.6 (CH), 38.1 (CH_2), 33.5, 26 (CH_2) ppm.

Synthesis of Mono-6-deoxy-6-azido-β-cyclodextrin (β-CD-N_3). In a 500 mL round-bottom flask β-cyclodextrin (20.0 g, 17.6 mmol) was suspended in 250 mL of 0.4 M sodium hydroxide (NaOH) aqueous solution. The flask was cooled to 0 °C in ice bath. TsCl (13.4 g, 70.3 mmol) was added in slow portions over 10 min. After 45 min of stirring at 0 °C, the precipitate was removed by filtration and the pH of the filtrate was adjusted to 8.5 by dropping HCl aqueous solution. Then the mixture was stirred for 1 h at room temperature. The resulting white precipitate was recovered by filtration and washed three times with water. The final product was used to synthesize β-CD-N_3 directly after drying in a vacuum oven at 60 °C. β-CD-OTs (8.0 g, 6.2 mmol) was suspended in 100 mL of water. After heating to 80 °C, NaN_3 (2.0 g, 31.0 mmol) was added. The reaction mixture was stirred at 80 °C for overnight. The reaction solution was cooled to room temperature and precipitated in 800 mL of acetone. The resulting white precipitate was recovered by filtration and redissolved in 50 mL of water and precipitated again in acetone. The white solid was dried under vacuum at 60 °C for 2 days (6.8 g, yield: 95%).

^{1}H NMR ($(CD_3)_2SO$), 298 K, 400 MHz): δ 5.72 (br, 14H, OH-2,3), 4.88 (s, H, H-1), 4.83 (d, 6H, H-1), 4.57−4.40 (br, 6H, OH-6), 3.86−3.50 (br, 28H, H-3,5,6,6′), 3.32 (br, 14H, H-2,4 overlap with H_2O) ppm. FT-IR ν: 3316 (OH), 2924 (CH), 2160 (C−C), 2102 (N═N), 1644 (C═C), 1364 (OH), 1152 (CN), 1077 (OH), 1025 (CH), 945, 853, 756 (NH), 704 (CH) cm^{-1}.

Synthesis of β-Cyclodextrin Acrylate Monomer (CDAc). Mono-6-deoxy-6-azido-β-cyclodextrin (1 g, 0.86 mmol) and propargyl acrylate (0.19 g, 1.72 mmol) were dissolved in DMF (6 mL), a DMF solution of $CuSO_4·5H_2O$ (21.47 mg, 0.086 mmol), and (+)-sodium L-ascorbate (34.1 mg, 0.172 mmol) were added into the reaction solution. The reaction solution was transferred into a microwave tube and then irradiated in the microwave at 120 °C for 1 h. After precipitating the reaction mixture with acetone, 0.76 g of product was isolated (69% yield).

^{1}H NMR ($(CD_3)_2SO$), 298 K, 400 MHz): δ 8.11 (1H, CH), 6.12 (H, −CH), 5.83 (br, 14H, OH-2,3), 5.22 (H, −CH), 5.06 (2H, −CH_2), 4.78 (d, 6H, H-1), 4.51 (br, 6H, OH-6), 3.62 (br, 28H, H-3,5,6), 3.31 (br, 14H, H-2,4) ppm. FT-IR ν: 3320 (OH), 2924 (CH_2), 1720 (CdO), 1652 (CdC), 1160 (C−O−C), 1075 (OH), 1023 (C−O). MALDI-TOF m/z: Calcd for $C_{48}H_{75}N_3O_{36}$ ($M + Na^+$), 1293.02; found, 1293.14.

Synthesis of p((DMA)$_{10}$-r-(Adac)$_2$) Macro-RAFT Agent. 2-(((Dodecylthio)carbonothioyl)thio)propan-2-yl pentanoate (1 equiv), DMA (10 equiv), Adac (2 equiv), AIBN (0.01 equiv), and solvent (5 mL) were introduced in a Schlenk tube equipped with a magnetic stirrer and sealed with a rubber septum. The reaction solution was degassed by gentle bubbling of argon gas for 30 min, and then the Schlenk tube was sealed properly and the mixed solution was allowed to polymerize. After the confirmation of nearly full conversion according to GC, the polymerization reaction was stopped by cooling down and exposure to air. Subsequently, the reaction solution was diluted with 2.0 mL of THF and then purified by precipitation in cold diethyl ether twice. After the filtration, the obtained polymer was dried in vacuo and characterized via ^{1}H NMR and DMF SEC analysis.

Synthesis of Well-Defined Triblock Copolymers. RAFT polymerization reactions were carried out in the presence of p((DMA)$_{10}$-r-(Adac)$_2$) as a RAFT agent, V-501 as an initiator in the water−DMF mixture at 70 °C. In order to polymerize a second block, a Schlenk tube was charged with DMA and ManAcm monomers (in total 24 equiv), macro-RAFT agent (1 equiv), V-501 (0.01 equiv), and water (2.0 mL) were degassed by gentle bubbling of argon gas for 30 min. During the polymerization, samples were withdrawn from the polymerization medium using a degassed syringe for GC and ^{1}H NMR to determine monomer conversions. When both monomers reached to nearly full conversion, the predegassed solution of DMA and CDAc (DMA/CDAc = 10:2) in DMF was added into the Schlenk tube. The reaction was stopped by cooling down, and then the reaction mixture was dialyzed against a mixture of distilled water and methanol for 3 days, while changing the water at least three times. The final product was freeze-dried under vacuum and characterized by ^{1}H NMR and DMF SEC.

Single-Chain Folding Studies. The diffusion coefficient of the obtained glycopolymers was measured using DOSY NMR at different concentrations in order to determine the necessary concentration for the single-chain regime. 2D NOESY NMR and DLS experiments at 25 °C and 70 °C were carried out at the calculated concentration. In order to open the single-chain folding structure, 1-aminoadamantane hydrochloride (1 mg) was added into solutions and then heated up 70 °C. Subsequently, it was allowed to cool down again and DLS was measured at 25 °C.

Turbidimetry Assay. A solution of 60 μM ConA in HBS buffer solution was prepared fresh before the assay. Turbidity measurements were performed by adding 350 μL of the ConA solution to a dry quartz microcuvette and put into the holder of UV−visible spectrophotometry at a certain temperature for 1 min. A solution of the ligand in HBS buffer (350 μL at 320 μM) was added into the cuvette via a pipet, the absorbance of the mixture was quickly recorded at 420 nm for 15 min every 0.12 s.

Surface Plasmon Resonance. The extent of interaction between the glycopolymers and lectins were performed on a BIAcore 2000 system (GE Healthcare). DC-SIGN, DC-SIGNR, and Dectin-1 (0.005 mg/mL) were immobilized via a standard amino coupling protocol onto a CM5 sensor chip that was activated by flowing a 1:1 mixture of 0.1 M *N*-hydroxysuccinimide and 0.1 M *N*-ethyl-*N*′-(dimethylaminopropyl)carbodiimide over the chip for 5 min at 25 °C at a flow rate of 5 μL/min after the system equilibration with HEPES filtered buffer (10 mM HEPES pH 7.4, 150 mM NaCl, 5 mM $CaCl_2$). Subsequently, channels 1 (blank), 2, 3, and 4 were blocked by following a solution of ethanolamine (1 M pH 8.5) for 10 min at 5 μL/min to remove remaining reactive groups on the channels. Sample solutions were prepared at varying concentrations (1000 nM to 62 nM) in the same HEPES buffer to calculate the binding kinetics. Sensorgrams for each glycopolymer concentration were recorded with a 300 s injection of polymer solution (on period) followed by 150 s of buffer alone (off period). Regeneration of the sensor chip surfaces was performed using 10 mM HEPES pH 7.4, 150 mM NaCl, 10 mM EDTA, and 0.01% P20 surfactant solution. Kinetic data was evaluated using a single set of sites (1:1 Langmuir binding) model and also Biavalent model in the BIAevalulation 3.1 software.

RESULTS AND DISCUSSION

Synthesis of D-Mannose Acrylamide Glycomonomer (ManAcm). Acrylamide derivatives can be polymerized via

DOI: 10.1021/acs.biomac.8b00600
Biomacromolecules 2018, 19, 3040−3047

Scheme 1. Schematic Representation of the Synthesis of Sequence Controlled Triblock Copolymers, And a Representation of the Formation of Single-Chain Folding in Highly Diluted Aqueous Solution[a]

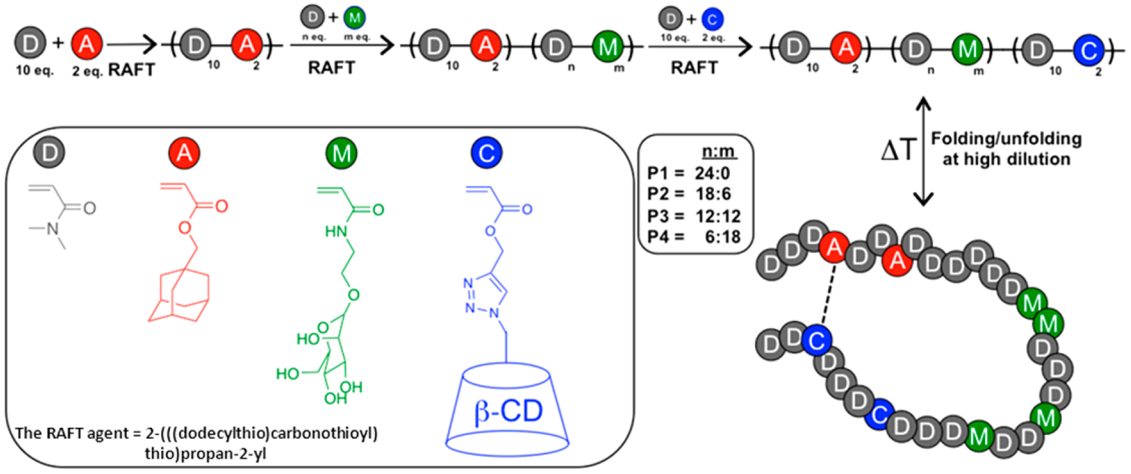

[a]The monomers used are **D**: *N*,*N*-dimethylacrylamide (grey), **A**: adamantyl-acrylate (red), **M**: D-mannose ethyl acrylamide (green), and **C**: *β*-CD acrylate (blue). The monomer ratios of D, A and D, C used in the first and third block are constant (10:2), while the ratio of *N*,*N*-dimethylacrylamide **D** and D-mannose ethyl acrylamide **M** in the middle block are varied as 24:0 (**P1**), 18:6 (**P2**), 12:12 (**P3**), and 6:18 (**P4**).

RAFT process to create complex high-order multiblock copolymers in a short polymerization time in one-pot reaction. Acrylamide monomers have a high propagation rate coefficient in aqueous solutions. In this work, *N*,*N*-dimethylacrylamide (DMA) was chosen to design triblock copolymers in which each block carries different functional moieties. Therefore, D-mannose acrylamide glycomonomer was synthesized according to previously published reports and used further for copolymerization with DMA. Mannosylated monomer tetra-*O*-acetyl-D-1-mannopyranosyl hydroxylethyl acrylamide was prepared by the reaction of *N*-hydroxyethyl acrylamide with D-mannose pentaacetate using boron trifluoride diethyl etherate ($BF_3{-}OEt_2$) as the activating agent. First, D-mannose pentaacetate was synthesized successfully and then used for the reaction with *N*-hydroxyethyl acrylamide. The reaction solution was sonicated for 90 min. After washing with brine, the solvent was removed under reduced pressure to obtain an off-white sticky crude product, which was used directly without any further purification to synthesize 2-(D-manosyloxy) hydroxylethyl acrylamide. The protection of acetyl groups was carried out in the presence potassium carbonate (K_2CO_3) in methanol (MeOH). The reaction was followed by thin-layer chromatography (TLC). After the neutralization of the reaction solution using Amberjet 1200H (H^+) cation exchange resin, the crude product was purified by column chromatography with 32% yield. The ManAcm structure was confirmed by ^{1}H NMR and ^{13}C NMR (Figure S1), and ESI-MS spectra showed a clear peak at 277.15 *m*/*z* that corresponds to the calculated molecular weight of the glycomonomer at 277.12 *m*/*z*.

Synthesis of Adamantane Acrylate Monomer (AdAc). In order to incorporate adamantyl functional groups into the polymers, adamantane acrylate was synthesized via esterification of 1-adamantane methanol with acryloyl chloride in THF overnight in the presence of triethlyamine (Et_3N; Scheme S2). The reaction was monitored by ^{1}H NMR. Esterification was confirmed by the appearance of the vinyl groups at 5.8−6.4 ppm and formation of ester protons at 3.8 ppm.

Synthesis of *β*-Cyclodextrin Acrylate Monomer (CDAc). Ritter and co-workers achieved synthesis of *β*-cyclodextrin methacrylate using CuAAC click chemistry and polymerization by free-radical polymerization (Scheme S4).[30] The CuAAC click reaction between *β*-CD-N_3 and propargyl acrylate was carried out in the presence of $CuSO_4{\cdot}5H_2O$ and (+)-sodium L-ascorbate as a catalyst system in DMF. The solution was irradiated at 120 °C in the microwave for an hour and the reaction was monitored, and products confirmed by ^{1}H NMR, FT-IR, and MALDI-ToF MS. The disappearance of the azide stretch signal at 2095 cm^{-1} allowed us to follow completion of the click reaction by FT-IR. The appearance of a peak at 8.1 ppm is consistent with formation of a triazole ring, and confirmed the new structure by ^{1}H NMR (Figure S3). Moreover, the MALDI-ToF MS spectrum showed peaks corresponding to the fully substituted product at 1309 (*m*/*z*). All these data are consistent with successful synthesis of *β*-cyclodextrin acrylate at high purity.

Synthesis of p($(DMA)_{10}$-*r*-$(AdAc)_2$) Macro-RAFT Agent. Random copolymerization of DMA and AdAc was performed to prepare water-soluble macro-RAFT agent for the further polymerization reactions (Scheme 1). The polymerization was carried out in 1,4-dioxane at 70 °C, with 2-(((dodecylthio)-carbonothioyl)thio)propan-2-yl pentanoate and 2,2′-azobis(2-methyl-propionitrile) (AIBN) as chain transfer agent (CTA) and radical initiator, respectively. Briefly, a Schlenk tube was charged with targeted monomers (DMA/AdAc = 10:2), CTA (1 equiv), AIBN (0.01 equiv), and the solvent, which had been previously degassed by gentle bubbling of argon gas for 30 min. The reaction was monitored to completion within 2 h according to GC, following which the tube was cooled with liquid nitrogen. The polymer was precipitated in cold hexane twice before characterization by SEC (eluent/DMF) and ^{1}H NMR. The SEC trace of the polymer yielded an M_n = 1500 g·mol^{-1} and $Đ$ = 1.14 according to PMMA calibration standards and did not show any shoulder or tailing. Moreover, the ^{1}H NMR spectrum revealed quantitative recovery of the copolymer after purification.

Synthesis of Well-Defined Triblock Copolymers. The p($(DMA)_{10}$-*r*-$(AdAc)_2$) was employed as macro-RAFT agent to synthesize triblock coglycopolymers. The RAFT polymerization of second and third blocks was performed in one-pot

DOI: 10.1021/acs.biomac.8b00600
Biomacromolecules 2018, 19, 3040−3047

chain extension reactions. Second block syntheses consisted of different ratios of DMA and ManAcm monomers, while all third blocks contained the same ratio of DMA and CDAc monomers (DMA/CDAc = 10:2). The second block RAFT polymerization was carried out in the presence of water-soluble 4,4′-Azobis(4-cyano-pentanoic acid) (V-501) radical initiator in water at 70 °C. The time to achieve quantitative monomer conversions increased when higher molar ratio of ManAcm was used. Chain extension of the third block was carried out in DMF/H_2O. The mixture of degassed DMA and CDAc monomers, initiator, and solvent was added via gastight syringe to the polymerization medium. Long reaction times were employed to ensure that conversions were close to completion. The necessary amount of initiator added for the third block polymerization was calculated according to the following formula;

$$m_{\text{V-501 remaining}} = m_{\text{V-501 total}} \times 2fe^{-k_d t} \times (1 - f_c/2)$$

where f = 0.5, f_c = 0, k_d = 1.9 × 10^{-5} s^{-1}, and t = polymerization time. The $[\text{Macro-RAFT agent}]_0/[\text{V-501}]_0$ ratio was kept at 100:1 to preserve high chain-end fidelity. It is important that at lower initiator concentrations the polymerization reaction requires a longer reaction time to reach full conversion.

Even though full consumption of monomers for each block was achieved, the conversion of CDAc remained lower than 76%, possibly because of the sterically demanding structure of the β-cyclodextrin ring. However, DMF SEC traces showed successful chain growth with peak shifts to lower retention time with the addition of each block (Figures 1 and S8). A small amount tailing in the low molar mass range after the third block polymerization is likely to be due to some dead polymer chains, but the final dispersity of the triblock copolymers was relatively narrow ($Đ$ = 1.18−1.24). As expected, the molar masses measured by SEC were higher than theoretical molar mass, but this is likely to be due to the PMMA calibration standards which have a different structure, and hence a different hydrodynamic volume in DMF. Thus, **P1**−**P4** were prepared using different ratio of *N*,*N*-dimethylacrylamide **D** and D-mannose ethyl acrylamide **M** in the middle block as 24:0 (**P1**), 18:6 (**P2**), 12:12 (**P3**), and 6:18 (**P4**).

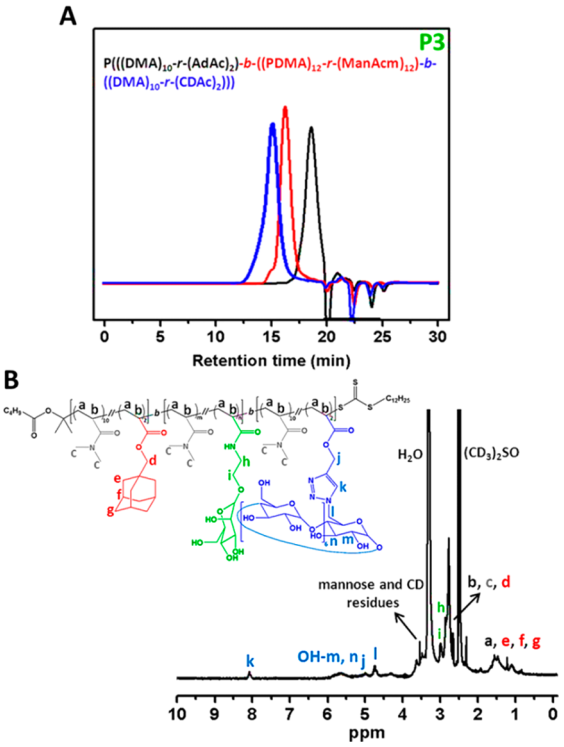

Figure 1. (A) SEC traces of **P3** via refractive index (RI) detector; (B) ^{1}H NMR analysis of **P3**.

Reversible Single-Chain Folding Studies of the Triblock Glycopolymers. As mentioned in the introduction, single-chain folded architectures can be created using both selective point folding, or repeat unit folding approaches. The selective point folding approach enables polymer chains to be folded into relatively controlled shapes with good accuracy. In contrast, the repeat unit folding approach provides less-defined folding structures. However, it is much easier to achieve repeat unit folding collapses than selective point folding collapses. We decided to study single-chain folding using our glycopolymers to investigate the influence of folded architecture on recognition by different lectins. The diffusion coefficient of each glycopolymer was measured at a series of concentrations using diffusion ordered spectroscopy (DOSY) NMR. The diffusion coefficient decreased with increasing concentration (Figure S9), which can be interpreted as the formation intermolecular aggregates. We then showed that single-chain folding of the triblock copolymers was achieved most effectively in highly diluted aqueous solution, below a concentration of 0.40 mM approximately. We also noted that the diffusion coefficient increased with higher ratios of sugar moieties on the polymer. This may be due to higher water solubility of sugar moieties over that of DMA moieties in water.

After optimizing single-chain folding, samples were prepared in D_2O for NMR. Product architecture was monitored via 2D nuclear overhauser enhancement spectroscopy (NOESY) NMR and dynamic light scattering (DLS). The 2D NOESY NMR spectra confirmed the cross-correlation signals between the protons of the CD cavity and the adamantane protons (Figure 2). The Adamantane protons between 1.52 and 2.02 ppm and the inner CD protons between 3.65 and 3.92 ppm presented clear cross-correlation signals. However, 2D NOESY NMR spectroscopy is not sufficiently diagnostic to confirm folded structures unambiguously. Therefore, DLS measurements were performed to measure mean hydrodynamic diameters (D_h, the volume weight diameter of the distribution) for further evidence of folded single-chain polymers. The D_h values were measured as 5.4−6.2 nm at 25 °C (Table S2). The biggest particles were found for **P1** (6.2 nm), **P4** has relatively the smallest size (5.4 nm). Additionally, DLS results showed that D_h values increased dramatically with increasing concentration, consistent with the formation of interchain assemblies of polymers or aggregations.

Previous studies have shown that the host−guest interactions between CD and adamantane can be reopened at high temperatures.[15−31] Therefore, copolymers were reanalyzed at 70 °C and the results show that D_h values for **P3** increased to approximately 11.3−12.2 nm, illustrating that the self-folding process is completely reversible (Figure 2). Temperature controlled unfolded copolymers were also followed via 2D NOESY NMR, studying the absence of cross-correlation signals (Figure 2). The interchain associations at high concentrations were reduced or reversed at 70 °C according

DOI: 10.1021/acs.biomac.8b00600
Biomacromolecules 2018, 19, 3040−3047

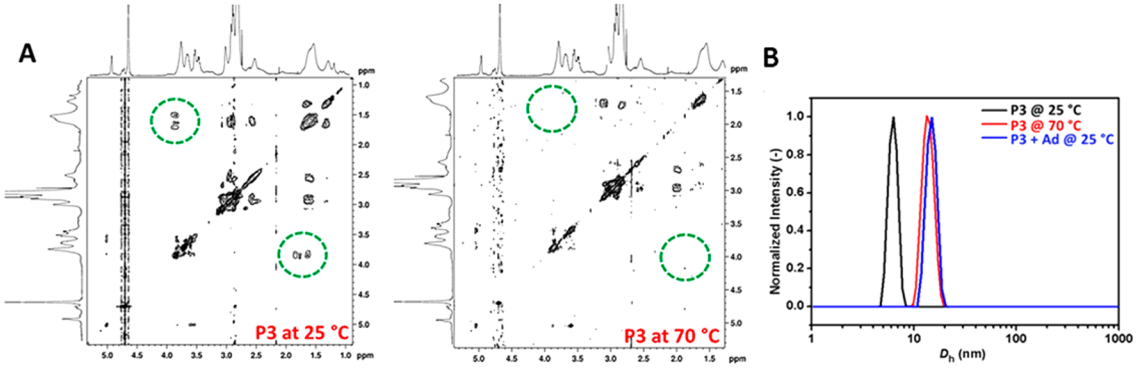

Figure 2. (A) 2D NOESY NMR spectra of **P3** at 25 and 70 °C; (B) Number-weighted size distributions of **P3** in aqueous solution (0.40 mM) at 25 and 70 °C.

to DLS (Figure S11). When the solution was cooled to ambient temperature, the D_h of the triblock copolymers again decreased to between 5.2 and 6.6 nm, which is in good agreement with the initial single-chain folded structure values (Figures 2 and S11). These evidence are quite important as it aids to prove that the folding behavior of glycopolymers can be easily controlled reversibly by adjusting the temperature of the solution. Barner-Kowollik and co-workers demonstrated displacement of adamantane moieties by providing competitive guest molecules and heating.[15] Glycocopolymer chains presented here have also unfolded successfully, and DLS results confirmed that the mean hydrodynamic diameter of the single-chain folding glycopolymers increased to 12.5−14.1 nm. Consequently, reversible folding of single-chain glycopolymer structures was achieved in dilute aqueous solution, and that this behavior can be controlled by either temperature or concentration.

Lectin Binding Studies. Carbohydrate-binding proteins (lectins) are important for many biological processes. Different lectins exhibit high specificity for sugar moieties.[32] If synthetic glycopolymers are to prove useful biomedical tools, they must be able to mimic and drive specific biological activities.[33−36] Therefore, we investigated the binding ability of folded and unfolded single-chain glycopolymer against the lectins Concanavalin A (ConA; Figure 3), DC-SIGN, and DC-SIGNR (Figure 4). ConA is a tetramer at neutral pH with high binding affinity for mannose and it has been widely studied in the literature as a model lectin to prove glycopolymer interactions. Therefore, it is a useful model lectin for investigating the multivalent binding of the folded glycopolymers.[37] For more detailed analysis, the interactions of these folded and unfolded glycopolymer structures with lectins were analyzed by using SPR. DC-SIGN and the closely related DC-SIGNR bind specifically to mannose containing glycans as reported previously.[38−40]

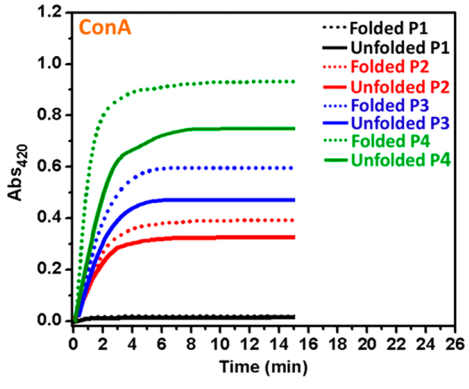

Figure 3. Turbidity measurements monitor the influence of folded structure on agglutinations with the lectin ConA.

Turbidimetry Assay. ConA was dissolved (approximately 60 μM) in HBS buffer and then transferred into a dry quartz microcuvette. A solution of the copolymer (320 μM) was added in HBS buffer and the A_{420} recorded for 15 min.[41] Glycopolymer **P1** lacking mannose moieties was used as a control and did not show any binding to ConA (Figure 3), while all other glycopolymers (**P2**−**P4**) induced rapid turbidity. In order to investigate the binding differences between single-chain folded and unfolded structures, unfolded solution was prepared by addition of 1-aminoadamantane hydrochloride and heating to 70 °C. When cooled to 25 °C, it was used immediately for the binding measurement. Folding enhanced binding significantly for all the maltose-bearing single-chain glycopolymers. Glycopolymer **P4** with the highest density of mannose residues showed the strongest binding with ConA. These results indicated that folding the single-chain has a crucial influence on interaction kinetics with proteins.

Surface Plasmon Resonance (SPR) Measurements. In order to investigate the interactions between different C-type lectins and glycopolymers with different carbohydrate density and folded structure detailed kinetic experiments were performed. According to the SPR measurements, glycopolymers **P2**−**P4** bound to DC-SIGN and DC-SIGNR strongly and selectively (Figure 4). As expected, **P1** with no mannose moieties did not present any binding, and also none of the mannose glycopolymers interacted with Dectin-1, which is a lectin specifically binds to β-glucans (Figure S14). These observations proved that the mannose glycopolymers are bound selectively rather than unspecific interactions on the SPR chip. Importantly, the SPR results also confirmed that folded single-chain structures enhanced the interaction notably for glycopolymers **P2**−**P4**. In particular, folded structure of **P4** appeared to exhibit the strongest binding with both DC-SIGN and DC-SIGNR. In all cases the sensorgrams indicate that the binding is multivalent, exhibiting initial rapid binding followed by a second phase of slower kinetics. These features are likely caused by initial high affinity binding of a mannose unit to one lectin site, increasing the mass on the chip surface. However, given the proximity of adjacent binding sites on the lectin tetramer, subsequent binding is most likely between already-bound glycopolymer and neighboring sites, causing no further

DOI: 10.1021/acs.biomac.8b00600
Biomacromolecules 2018, 19, 3040−3047

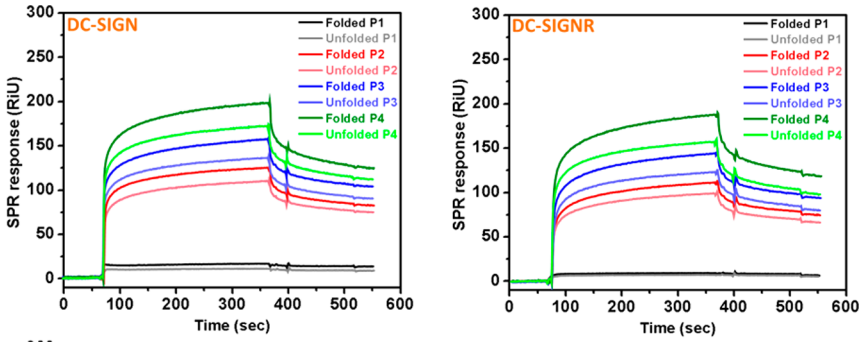

Figure 4. Comparison of the binding of folded and unfolded glycopolymers to the lectins DC-SIGN and DC-SIGNR. All polymers were presented at a concentration of 1 μM.

Table 1. Kinetic Data of Folded and Unfolded Glycopolymers Binding to DC-SIGN[a]

polymer	ligand	k_{a1} (1/Ms)	k_{d1} (1/s)	K_{D1} (nM)	k_{a2} (1/RUs)	k_{d2} (1/s)	R_{max} (RU)	Chi2 value
P1	folded							
P1	unfolded							
P2	folded	1.39×10^4	2.44×10^{-5}	1.76	3.12×10^{-2}	3.47×10^{-2}	115	16.2
P2	unfolded	1.09×10^4	1.88×10^{-5}	1.72	2.96×10^{-2}	3.06×10^{-2}	106	17.4
P3	folded	2.30×10^4	3.16×10^{-5}	1.37	3.89×10^{-2}	5.24×10^{-2}	141	22.3
P3	unfolded	2.16×10^4	3.01×10^{-5}	1.39	3.55×10^{-2}	4.31×10^{-2}	128	24.8
P4	folded	2.84×10^5	5.12×10^{-5}	1.80	4.33×10^{-2}	8.25×10^{-3}	172	21.5
P4	unfolded	2.52×10^4	4.67×10^{-5}	1.85	3.12×10^{-2}	6.91×10^{-2}	153	27.3

[a]Binding was measured by SPR and the data analyzed using a bivalent model.

increase in the total mass on the surface as evident from the flatter phase of binding in the sensorgrams.

Furthermore, kinetic experiments titrating polymer against immobilized lectin show clearly that it is not possible to achieve a good fit using 1:1 Langmuir kinetics, which is quite often used in this field to calculate the binding kinetics. This indicates that the binding is not consistent with single site binding. Therefore, a much better fit is achieved with the bivalent binding site model, consistent with multivalent binding (Tables 1 and S2). It is not surprising that the initial affinity value is similar for all polymers because the initial binding is equivalent in each case. However, the nanomolar affinity values appear high compared with data for monomer binding affinities, which are generally in the micromolar range. This suggests that second and higher order binding events follow at adjacent sites very rapidly, making dissociation unlikely and reducing the dissociation rates. Similar nanomolar kinetics have been reported for multivalent ligands and the *Entamoeba histolytica* lectin using different biophysical techniques,[28] and enhancement of affinity on DC-SIGN by multivalent mannose moieties and has been shown to be attributed to multiple modes of binding as well as adjacent site enhancement.[29,11] According to SPR kinetic binding data, there is little difference in equilibrium dissociation binding constants (K_{D1}) for folded and unfolded glycopolymers. The unfolded **P2** represented a little bit higher binding affinity than the folded **P2** because of the lower dissociation rate constant in contrast to other folded and unfolded glycopolymers. The results indicated that the folding of single-chain glycopolymers enhance binding with proteins and suggest that this ordering of the carbohydrate residues significantly improves binding compared to the same polymer, but unfolded. Although the mechanism for such improved affinity remains unclear, it may be due to more favorable entropy, or more favorable disposition of second and higher order moieties to find adjacent binding sites.

CONCLUSION

In this study, well-defined triblock glycocopolymers bearing β-CD and adamantane for the host−guest interaction and also mannose residues for the interaction with lectins were synthesized via RAFT polymerization. The single-chain folding of glycopolymers and its reversion were monitored by 2D NOESY NMR and DLS. Folded single-chain glycocopolymer structures were achieved in aqueous solution under high dilution. Folded glycopolymers were unfolded at high temperatures and also by addition of a competitive guest molecule. Lectin binding assays of single-chain folded glycopolymers were performed using turbidimetry and SPR. The results strongly indicated that the folded glycopolymers enhanced the multivalent binding interaction compared to the unfolded glycopolymers and directly proves the unprecedented effect of secondary structures of polymers on biological applications.

ASSOCIATED CONTENT

Supporting Information

The Supporting Information is available free of charge on the ACS Publications website at DOI: 10.1021/acs.biomac.8b00600.

Experimental details and data (PDF).

AUTHOR INFORMATION

Corresponding Author

*E-mail: r.becer@qmul.ac.uk.

ORCID

C. Remzi Becer: 0000-0003-0968-6662

DOI: 10.1021/acs.biomac.8b00600
Biomacromolecules 2018, 19, 3040−3047

Notes

The authors declare no competing financial interest.

■ ACKNOWLEDGMENTS

This study is supported by Engineering and Physical Sciences Research Council (EPSRC, EP/P009018/1).

■ REFERENCES

(1) Dobson, C. M. *Nature* **2003**, *426* (6968), 884−890.
(2) Dill, K. A.; MacCallum, J. L. *Science* **2012**, *338* (6110), 1042−1046.
(3) Perrier, S. Polymer folding: ABC of molecular origami. *Nat. Chem.* **2011**, *3* (3), 194−196.
(4) Matyjaszewski, K. *Macromolecules* **2012**, *45*, 4015−4039.
(5) Moad, G. *Polym. Chem.* **2017**, *8*, 177−219.
(6) Nicolas, J.; Guillaneuf, Y.; Lefay, C.; Bertin, D.; Gigmes, D.; Charleux, B. *Prog. Polym. Sci.* **2013**, *38*, 63−235.
(7) Anastasaki, A.; Nikolaou, V.; Nurumbetov, G.; Wilson, P.; Kempe, K.; Quinn, J. F.; Davis, T. P.; Whittaker, M. R.; Haddleton, D. M. *Chem. Rev.* **2016**, *116*, 835−877.
(8) Hartweg, M.; Edwards-Gayle, C. J. C.; Radvar, E.; Collis, D.; Reza, M.; Kaupp, M.; Steinkoenig, J.; Ruokolainen, J.; Rambo, R.; Barner-Kowollik, C.; Hamley, I. W.; Azevedo, H. S.; Becer, C. R. *Polym. Chem.* **2018**, *9* (4), 482−489.
(9) Abdouni, Y.; Yilmaz, G.; Becer, C. R. *Macromol. Rapid Commun.* **2017**, *38* (24), 1700212.
(10) Lavilla, C.; Yilmaz, G.; Uzunova, V.; Napier, R.; Becer, C. R.; Heise, A. *Biomacromolecules* **2017**, *18* (6), 1928−1936.
(11) Mitchell, D. A.; Zhang, Q.; Voorhaar, L.; Haddleton, D.; Herath, S.; Gleinich, A. S.; Randeva, H. S.; Crispin, M.; Lehnert, H.; Wallis, R.; Patterson, S.; Becer, C. R. *Chem. Sci.* **2017**, *8* (10), 6974−6980.
(12) Altintas, O.; Gerstel, P.; Dingenouts, N.; Barner-Kowollik, C. *Chem. Commun.* **2010**, *46* (34), 6291−6293.
(13) Altintas, O.; Rudolph, T.; Barner-Kowollik, C. *J. Polym. Sci., Part A: Polym. Chem.* **2011**, *49* (12), 2566−2576.
(14) Willenbacher, J.; Altintas, O.; Roesky, P. W.; Barner-Kowollik, C. *Macromol. Rapid Commun.* **2014**, *35* (1), 45−51.
(15) Willenbacher, J.; Schmidt, B. V. K. J.; Schulze-Suenninghausen, D.; Altintas, O.; Luy, B.; Delaittre, G.; Barner-Kowollik, C. *Chem. Commun.* **2014**, *50* (53), 7056−7059.
(16) Lutz, J.-F. *Polym. Chem.* **2010**, *1* (1), 55−62.
(17) Schmidt, B. V. K. J.; Fechler, N.; Falkenhagen, J.; Lutz, J.-F. *Nat. Chem.* **2011**, *3* (3), 234−238.
(18) Shishkan, O.; Zamfir, M.; Gauthier, M. A.; Borner, H. G.; Lutz, J.-F. *Chem. Commun.* **2014**, *50* (13), 1570−1572.
(19) Inoue, Y.; Kuad, P.; Okumura, Y.; Takashima, Y.; Yamaguchi, H.; Harada, A. *J. Am. Chem. Soc.* **2007**, *129* (20), 6396−6397.
(20) Altintas, O.; Krolla-Sidenstein, P.; Gliemann, H.; Barner-Kowollik, C. *Macromolecules* **2014**, *47* (17), 5877−5888.
(21) Altintas, O.; Lejeune, E.; Gerstel, P.; Barner-Kowollik, C. *Polym. Chem.* **2012**, *3* (3), 640−651.
(22) Fan, W.; Tong, X.; Yan, Q.; Fu, S.; Zhao, Y. *Chem. Commun.* **2014**, *50* (88), 13492−13494.
(23) Glassner, M.; Oehlenschlaeger, K. K.; Gruendling, T.; Barner-Kowollik, C. *Macromolecules* **2011**, *44* (12), 4681−4689.
(24) Song, W.; Wang, Y.; Qu, J.; Lin, Q. *J. Am. Chem. Soc.* **2008**, *130* (30), 9654−9655.
(25) Mueller, J. O.; Guimard, N. K.; Oehlenschlaeger, K. K.; Schmidt, F. G.; Barner-Kowollik, C. *Polym. Chem.* **2014**, *5* (4), 1447−1456.
(26) Yang, H.; Yuan, B.; Zhang, X.; Scherman, O. A. *Acc. Chem. Res.* **2014**, *47* (7), 2106−2115.
(27) Schmidt, B. V. K. J.; Hetzer, M.; Ritter, H.; Barner-Kowollik, C. *Prog. Polym. Sci.* **2014**, *39* (1), 235−249.
(28) Séon, L.; Parat, A.; Gaudière, F.; Voegel, J.-C.; Auzély-Velty, R.; Lorchat, P.; Coche-Guérente, L.; Senger, B.; Schaaf, P.; Jierry, L.; Boulmedais, F. *Langmuir* **2014**, *30* (22), 6479−6488.
(29) Zhang, Y.; Tu, Q.; Wang, D.-E.; Chen, Y.; Lu, B.; Yuan, M.-S.; Wang, J. *New J. Chem.* **2013**, *37* (8), 2358−2368.
(30) Munteanu, M.; Choi, S.; Ritter, H. *Macromolecules* **2008**, *41*, 9619−9623.
(31) Schmidt, B. V. K. J.; Hetzer, M.; Ritter, H.; Barner-Kowolli, C. *Macromolecules* **2013**, *46*, 1054−1065.
(32) Yilmaz, G.; Uzunova, V.; Hartweg, M.; Beyer, V.; Napier, R.; Becer, C. R. *Polym. Chem.* **2018**, *9* (5), 611−618.
(33) Yilmaz, G.; Guler, E.; Geyik, C.; Demir, B.; Ozkan, M.; Odaci Demirkol, D.; Ozcelik, S.; Timur, S.; Becer, C. R. *Mol. Sys. Des. & Eng.* **2018**, *3* (1), 150−158.
(34) Liu, R.; Patel, D.; Screen, H. R. C.; Becer, C. R. *Bioconjugate Chem.* **2017**, *28* (7), 1955−1964.
(35) Yilmaz, G.; Demir, B.; Timur, S.; Becer, C. R. *Biomacromolecules* **2016**, *17* (9), 2901−2911.
(36) Yilmaz, G.; Messager, L.; Gleinich, A. S.; Mitchell, D. A.; Battaglia, G.; Becer, C. R. *Polym. Chem.* **2016**, *7* (41), 6293−6296.
(37) Gou, Y.; Geng, J.; Richards, S.-J.; Burns, J.; Becer, C. R.; Haddleton, D. M. *J. Polym. Sci., Part A: Polym. Chem.* **2013**, *51* (12), 2588−2597.
(38) Zhang, Q.; Collins, J.; Anastasaki, A.; Wallis, R.; Mitchell, D. A.; Becer, C. R.; Haddleton, D. M. *Angew. Chem., Int. Ed.* **2013**, *52* (16), 4435−4439.
(39) Becer, C. R.; Gibson, M. I.; Geng, J.; Ilyas, R.; Wallis, R.; Mitchell, D. A.; Haddleton, D. M. *J. Am. Chem. Soc.* **2010**, *132* (43), 15130−15132.
(40) Zhang, Q.; Su, L.; Collins, J.; Chen, G.; Wallis, R.; Mitchell, D. A.; Haddleton, D. M.; Becer, C. R. *J. Am. Chem. Soc.* **2014**, *136* (11), 4325−4332.
(41) Cairo, C. W.; Gestwicki, J. E.; Kanai, M.; Kiessling, L. L. *J. Am. Chem. Soc.* **2002**, *124* (8), 1615−1619.

DOI: 10.1021/acs.biomac.8b00600
Biomacromolecules 2018, 19, 3040−3047